Influence of optical phonons on the electronic mobility in a strained wurtzite AlN/GaN heterojunction under hydrostatic pressure[*]

Zhou Xiaojuan(周晓娟) and Ban Shiliang(班士良)[†]

(Department of Physics, School of Physical Science and Technology, Inner Mongolia University, Hohhot 010021, China)

Abstract: A variational method combined with solving the force balance equation is adopted to investigate the influence of strain and hydrostatic pressure on electronic mobility in a strained wurtzite AlN/GaN heterojunction by considering the scattering of optical-phonons in a temperature ranges from 250 to 600 K. The effects of conduction band bending and an interface barrier are also considered in our calculation. The results show that electronic mobility decreases with increasing hydrostatic pressure when the electronic density varies from 1.0×10^{12} to 6.5×10^{12} cm^{-2}. The strain at the heterojunction interface also reduces the electronic mobility, whereas the pressure influence becomes weaker when strain is taken into account. The effect of strain and pressure becomes more obvious as temperature increases. The mobility first increases and then decreases significantly, whereas the strain and hydrostatic pressure reduce this trend as the electronic density increases at a given temperature (300 K). The results also indicate that scattering from half space phonon modes in the channel side plays a dominant role in mobility.

Key words: hydrostatic pressure; strained AlN/GaN heterojunction; electronic mobility; optical-phonon scattering
DOI: 10.1088/1674-4926/30/8/082001   **PACC:** 6320K; 7210; 7340L

1. Introduction

With the development of technology, group III nitride semiconductors such as AlN and GaN have attracted a great deal of attention since the 1970s due to their advantages such as high output power, high conversion efficiency, high linearity and low power consumption. In recent years, the hydrostatic pressure effect in nitride semiconductors and their low-dimensional systems has been discussed in many theoretical and experimental works. Wagner *et al.*[1] studied the dielectric constants and lattice vibration frequencies under hydrostatic pressure in wurtzite and zincblende GaN, AlN by using the *ab initio* calculation method. The result indicated that the dielectric constants decrease and the phonon frequencies increase as hydrostatic pressure increases. Goñi *et al.*[2] investigated experimentally the hydrostatic pressure modification on the phonon modes in GaN and AlN, and obtained the same conclusion as Wagner. Consejo *et al.*[3] measured the concentration and mobility of a two-dimensional electron gas (2DEG) in AlGaN/GaN heterostructures under hydrostatic pressure, and the results showed that the electron concentration increases, whereas the mobility decreases with increasing pressure. More recently, an *ab initio* calculation method was adopted by Łepkowski to investigate the elastic constants as a function of hydrostatic pressure in group III nitride materials, who concluded that the elastic constants of materials increase as pressure increases[4]. The accumulation of data in previous work is helpful to study the hydrostatic pressure effect on the mobility of a 2DEG in wurtzite AlN/GaN heterostructures.

Jia and Ban[5] investigated the electronic mobility in wurtzite AlN/GaN quantum wells (QWs) under hydrostatic pressure. It was shown that there is a large reduction of the total electronic mobility in wurtzite QWs compared with that in zincblende ones due to structural anisotropy. Unfortunately, the strain effect was neglected in their calculation.

The lattice mismatch between the two materials is still relatively large in low-dimensional heterostructures of nitride semiconductors, even with hydrostatic pressure (the lattice mismatch is 2.4% in the AlN/GaN heterostructure), indicating that the strain effect is obvious and it should be considered in further study.

In this paper, a variational method combined with solving the force balance equation is adopted to investigate the scattering of optical-phonons on the mobility of a 2DEG in a strained wurtzite AlN/GaN heterojunction under hydrostatic pressure by taking energy band bending, the finite barrier and the tunneling effect of electrons into account.

2. Model and calculation

Let us consider a heterojunction consisting of two different wurtzite semiconductors, for which the channel side GaN denoted by material 1 is located at $z > 0$ and the barrier side AlN denoted by material 2 is located at $z < 0$, respectively. The z axis is collinear with the c-axis and perpendicular to the interface, and the direction parallel to the interface is denoted as //.

The finite self-consistent potential method used in

Ref. [6] is adopted here to model the system. The electrons are described by a ground-state wave function:

$$\psi_k(\rho, z) = \frac{1}{\sqrt{A}} \exp\left[i(k \cdot \rho)\right] \zeta(z), \tag{1}$$

with associated energy level $E_k = E_0 + \hbar^2 k^2 / 2m_{//}$. Here E_0 is the energy of an electron at ground state. $k = (k_x, k_y)$ and $\rho = (x, y)$ are the 2D momentum and coordinate vectors of the electron, respectively. The envelope function $\zeta(z)$ describes the localization of the electrons in the z direction and can be given by

$$\zeta(z) = \begin{cases} \zeta_1(z) = Bb^{1/2}(bz + \beta)\exp(-bz/2), & z > 0, \\ \zeta_2(z) = B'(b')^{1/2}\exp(b'z/2), & z < 0. \end{cases} \tag{2}$$

The average band mass defined above for an electron parallel to the x–y plane satisfies $m_{//} = m_{1//}m_{2//}/(m_{1//}p_2 + m_{2//}p_1)$. Here subscripts 1 and 2 correspond to the effective masses of the electron in GaN and AlN, respectively. The partial probabilities are $p_1 = \int_0^\infty |\zeta_1(z)|^2 dz$, and $p_2 = \int_{-\infty}^0 |\zeta_2(z)|^2 dz$ due to the electron penetration in each material. In Eq. (2), B, B' and β depend on the variational parameters b and b'.

The above envelope function can be obtained by solving the Schrödinger equation of the electron in the z direction:

$$-\frac{\hbar^2}{2}\frac{\partial}{\partial z}\frac{1}{m(z)}\frac{\partial}{\partial z}\zeta(z) + V(z)\zeta(z) = E_0\zeta(z), \tag{3}$$

where $m(z)$ is the position-dependent effective mass in the z direction of an electron; i.e., $m(z) = m_{1z}$ for $z > 0$, and $m(z) = m_{2z}$ for $z < 0$, and the heterojunction potential is given by

$$V(z) = V_0\theta(-z) + V_s(z) + V_d(z). \tag{4}$$

In Eq. (4), $\theta(-z)$ is the step function, and V_0 is the potential barrier height. According to the 65 : 20 principle[7], it is given by $V_0 = 0.765(E_{g2} - E_{g1})$, where E_{g1} and E_{g2} denote the energy gaps of materials 1 and 2, respectively. $V_s(z)$ and $V_d(z)$ are the contributions to the potential from electrons and depletion charges, respectively. They can be obtained by the following equations:

$$\frac{\partial}{\partial z}\varepsilon_0(z)\frac{\partial}{\partial z}V_s(z) = -4\pi e^2 n_s |\zeta(z)|^2, \tag{5}$$

$$\frac{\partial}{\partial z}\varepsilon_0(z)\frac{\partial}{\partial z}V_d(z) = -4\pi e^2 [n_A(z) - n_D(z)]. \tag{6}$$

Here, n_s is the area electron density. $\varepsilon_0(z)$ is the position-dependent static dielectric constant which equals ε_{01z} for $z > 0$, and ε_{02z} for $z < 0$, respectively. $n_A(z)$ and $n_D(z)$ are the position-dependent acceptor and donor concentrations. The ground-state energy in terms of the variational parameters b and b' will be obtained when one inserts Eqs. (2) and (4)–(6) into Eq. (3) as

$$E_0 = \langle T \rangle + \langle V_0 \rangle + \langle V_d \rangle + \langle V_s \rangle, \tag{7}$$

where

$$\langle T \rangle = \frac{\hbar^2}{2}\left[\frac{(Bb)^2\left(1 + \beta - \beta^2/2\right)}{2m_{1z}} - \frac{(B'b')^2}{4}m_{2z}\right], \tag{8}$$

$$\langle V_0 \rangle = V_0 B'^2, \tag{9}$$

$$\langle V_d \rangle = 4\pi e^2 n_D\left[-\frac{B'^2}{b'\varepsilon_{02z}} + \frac{B^2\left(6 + 4\beta + \beta^2\right)}{b\varepsilon_{01z}}\right], \tag{10}$$

$$\langle V_s \rangle = 4\pi e^2 n_s\left[-\frac{B'^2\left(1 - B'^2/2\right)}{b'\varepsilon_{02z}}\right.$$

$$\left.+ \frac{B^4\left(2\beta^4 + 12\beta^3 + 34\beta^2 + 50\beta + 33\right)}{4b\varepsilon_{01z}}\right]. \tag{11}$$

The variational envelope function $\zeta(z)$ can be obtained by minimizing energy $E_0 - \langle V_s \rangle/2$ with respect to b and b'.

For a single-heterojunction of wurtzite AlN/GaN, there are two distinct classes of optical-phonon modes: the interface (IF) and half space (HS) modes[8]. The IF modes appearing at the interface generate the following potential:

$$\varphi_{IF,q_{//}}(z) = -\left[\frac{4\pi\hbar L^{-2}}{\left|(\partial/\partial\omega_{IF})\left(\sqrt{\varepsilon_{1//}/\varepsilon_{1z}} - \sqrt{\varepsilon_{2//}/\varepsilon_{2z}}\right)\right|}\right]^{1/2}$$

$$\times \frac{1}{\sqrt{q_{//}}}\begin{cases} \exp\left(-\sqrt{\varepsilon_{1//}/\varepsilon_{1z}}\,q_{//}z\right), & z > 0, \\ \exp\left(\sqrt{\varepsilon_{2//}/\varepsilon_{2z}}\,q_{//}z\right), & z < 0, \end{cases} \tag{12}$$

and the potential of the HS modes is:

$$\varphi_{HS,q}(z) = -\left[\frac{4\pi\hbar L^{-3}}{\left|(\partial/\partial\omega_{HS})\left(\varepsilon_{1//}\sin^2\theta_1 + \varepsilon_{1z}\cos^2\theta_1\right)\right|}\right]^{1/2}$$

$$\times \frac{1}{\sqrt{q_{//}^2 + q_{1z}^2}}\frac{2}{\sqrt{\varepsilon_{1z}^2 q_{1z}^2 + \varepsilon_{2//}/\varepsilon_{2z}q_{//}^2}}$$

$$\times \begin{cases} \varepsilon_{1z}q_{1z}\cos(q_{1z}z) + \sqrt{\varepsilon_{2//}/\varepsilon_{2z}}\,q_{//}\sin(q_{1z}z), & z > 0, \\ \varepsilon_{1z}q_{1z}\exp\sqrt{\varepsilon_{2//}/\varepsilon_{2z}}\,q_{//}z, & z < 0. \end{cases} \tag{13}$$

In Eqs. (12) and (13), $q_{//}$ and q_z are the projections in the x–y plane and z direction of wave vector q for the phonon modes, respectively. The IF phonon frequency ω_{IF} can be obtained by the dispersion relation $\sqrt{\varepsilon_{1//}/\varepsilon_{1z}} - \sqrt{\varepsilon_{2//}/\varepsilon_{2z}} = 0$ with $\varepsilon_{1//}\varepsilon_{1z} > 0, \varepsilon_{2//}\varepsilon_{2z} > 0$ and $\varepsilon_{1z}\varepsilon_{2z} < 0$. The HS phonon frequency ω_{HS} can be obtained by $\omega_{HS}^2 = \omega_{zL}^2\cos^2\theta_1 + \omega_{//L}^2\sin^2\theta_1$. θ_1 is the angle between $(q_{//}, k_{1z})$ and the z axis. The direction-dependent dielectric functions $\varepsilon_{i//}(\omega_\lambda)$ and $\varepsilon_{iz}(\omega_\lambda)$ for the i-th material are given by

$$\varepsilon_{i//}(\omega_\lambda) = \varepsilon_{i//}^\infty\frac{\omega_\lambda^2 - \omega_{i//L}^2}{\omega_\lambda^2 - \omega_{i//T}^2}, \tag{14}$$

and

$$\varepsilon_{iz}(\omega_\lambda) = \varepsilon_{iz}^\infty\frac{\omega_\lambda^2 - \omega_{izL}^2}{\omega_\lambda^2 - \omega_{izT}^2}. \tag{15}$$

Here, index λ represents the IF and HS phonon modes, respectively.

According to the force-balance equation, the mobility of the 2DEG influenced by each branch of phonon modes is expressed as[9]

$$\frac{1}{\mu_\lambda} = \frac{2\hbar}{n_s e k_B T} \sum_q q_x^2 |M(\boldsymbol{q}, \lambda)|^2 \Pi_{02}(q_{//}, \omega_\lambda) \frac{e^{\hbar\omega_\lambda/k_B T}}{(1 - e^{\hbar\omega_\lambda/k_B T})^2}. \tag{16}$$

Then the total mobility can be obtained by $\mu^{-1} = \sum_\lambda \mu_\lambda^{-1}$. The electron–phonon interaction matrix in Eq. (16) can be written as

$$M(q, \lambda) = e \int \zeta^\dagger(z) \varphi_{\lambda,q}(z) \zeta(z) \, dz. \tag{17}$$

Π_{02} in Eq. (16) is the imaginary part of the zero-order two-dimensional density–density correlation function; it is expressed by

$$\Pi_{02}(q_{//}, \omega_\lambda) = \frac{A m_{//}}{\pi \hbar^3 q_{//}} \left(\frac{m_{//} k_B T}{2}\right)^{1/2}$$
$$\times [g(\phi_- - \phi_F) - g(\phi_+ - \phi_F)], \tag{18}$$

where

$$\phi_F = \frac{E_F}{k_B T}, \qquad \phi_\pm = \phi_F \frac{\left(\hbar\omega_\lambda m_{//} \pm \hbar^2 q_{//}^2/2\right)^2}{\hbar^4 k_F^2 q_{//}^2},$$

and $g(y) = \int_0^\infty \left\{[\exp(y+z) + 1] \sqrt{z}\right\}^{-1} dz$. Here, E_F and k_F are the Fermi-energy level and corresponding wave vector, respectively. They can be obtained by $E_F = \pi\hbar^2 n_s/m_{//}$ and $k_F = (2m_{//} E_F)^{1/2}/\hbar$.

According to Refs. [10, 11], the strain-dependent energy gaps of GaN and AlN under hydrostatic pressure can be described as

$$E_{g1} = E_{g1}(0) + 2(a_{11} + b_{11}) e_{1//}(P) + (a_{21} + b_{21}) e_{1z}(P) + \alpha_1 P, \tag{19}$$

$$E_{g2} = E_{g2}(0) + 2a_{12} e_{2//}(P) + a_{22} e_{2z}(P) + \alpha_2 P, \tag{20}$$

where α_1 and α_2 represent the pressure coefficients of GaN and AlN given in Table 2. $a_{1,i}$, $a_{2,i}$, $b_{1,i}$ and $b_{2,i}$ are the deformation potentials given in Ref. [10]. $E_{g1}(0)$ and $E_{g2}(0)$ are the strain-free energy gaps. The biaxial lattice-mismatch-induced strain tensors are given as

$$e_{1//}(P) = \frac{a_2(P) - a_1(P)}{a_1(P)}, \tag{21}$$

$$e_{2//}(P) = \frac{a_1(P) - a_2(P)}{a_2(P)}, \tag{22}$$

in which the lattice constants depend on hydrostatic pressure and are given by[12]

$$a_i(p) = a_i(0) \left(1 - \frac{P}{3B_{0i}}\right). \tag{23}$$

The bulk modulus in a wurtzite structure is given by the elastic constants C_{11i}, C_{12i}, C_{13i} and C_{33i}, and can be expressed as[13]

$$B_{0i} = \frac{(C_{11i} + C_{12i}) C_{33i} - 2C_{13i}^2}{C_{11i} + C_{12i} + 2C_{33i} - 4C_{13i}}. \tag{24}$$

From Hook's law the uniaxial and biaxial strain tensor ratio can be expressed by

$$\frac{e_{iz}(P)}{e_{i//}(P)} = \frac{C_{11i} + C_{12i} - 2C_{13i}}{C_{33i} - C_{13i}}. \tag{25}$$

The effective masses of an electron in the τ ($\tau = //, z$) direction can be calculated by[11]

$$\frac{m_0}{m_{i\tau}(P)} = 1 + \frac{C}{E_{gi}(P)}, \tag{26}$$

where C is a constant independent of pressure. The high frequency dielectric constant can be written as[14]

$$\frac{\partial \varepsilon_{i\tau}^\infty(P)}{\partial P} = -\frac{5\left(\varepsilon_{i\tau}^\infty - 1\right)}{3B_{0i}} (0.9 - f_I), \tag{27}$$

where f_I is the ionicity of the material under pressure. The static dielectric constants for the wurtzite structure are derived from the generalized Lyddane–Sachs–Teller relation

$$\varepsilon_{0i\tau} = \varepsilon_{i\tau}^\infty \left(\frac{\omega_{i\tau L}}{\omega_{i\tau T}}\right)^2. \tag{28}$$

The frequencies of longitudinal-optical (LO) and transverse-optical (TO) phonons affected by the strain can be written as[13]

$$\omega_{i\tau j} = \omega_{i\tau j}(0) + 2K_{i//j} e_{i//} + K_{izj} e_{iz}, \tag{29}$$

in which $K_{i//j}$ and K_{izj} are the strain coefficients given in Ref. [13] for phonon modes $j = $ LO, TO in the directions of $//$ and z, respectively. Furthermore, the hydrostatic pressure dependence of $\omega_{i\tau j}$ can be determined by the given mode-Grüneisen parameters[15]:

$$\gamma_{i\tau j} = B_{0i} \frac{1}{\omega_{i\tau j}} \frac{\partial \omega_{i\tau j}(P)}{\partial P}. \tag{30}$$

3. Results and discussion

The parameters used in our computation are listed in Tables 1 and 2, respectively. The results obtained by computation for wurtzite AlN/GaN heterojunctions are given by Figs. (1)–(4).
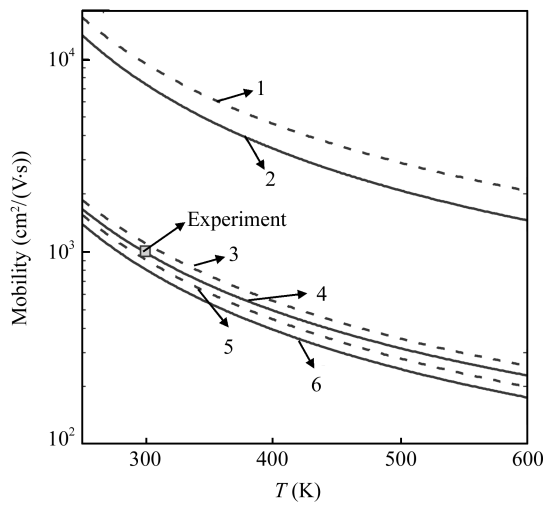
Figure 1 gives the contributions to the electronic mobility from each branch of the phonon modes for unstrained and strained heterojunctions as functions of temperature at hydrostatic pressure $P = 0$ kbar and electronic density $n_s = 2 \times 10^{12}$ cm^{-2}. It can be seen that the mobility obviously decreases when the strain at the interface is under consideration, and the reduction increases gradually with temperature. This phenomenon results from the complex effect of strain on the parameters of the materials, such as electronic effective masses, dielectric constants, and energy gaps. Our numerical computation indicates that the strain effect increases the energy gap in the channel (GaN), whereas it decreases it in the barrier (AlN). This change leads to a decrease of interface potential height and weakening of the bond to the 2DEG, so that the electrons penetrate into the barrier more easily than that without strain. This implies that scattering from the HS phonon modes in the

Table 1. Physical parameters of wurtzite GaN and AlN. The lattice constants are in units of angstrom, and the elastic constants in kbar.

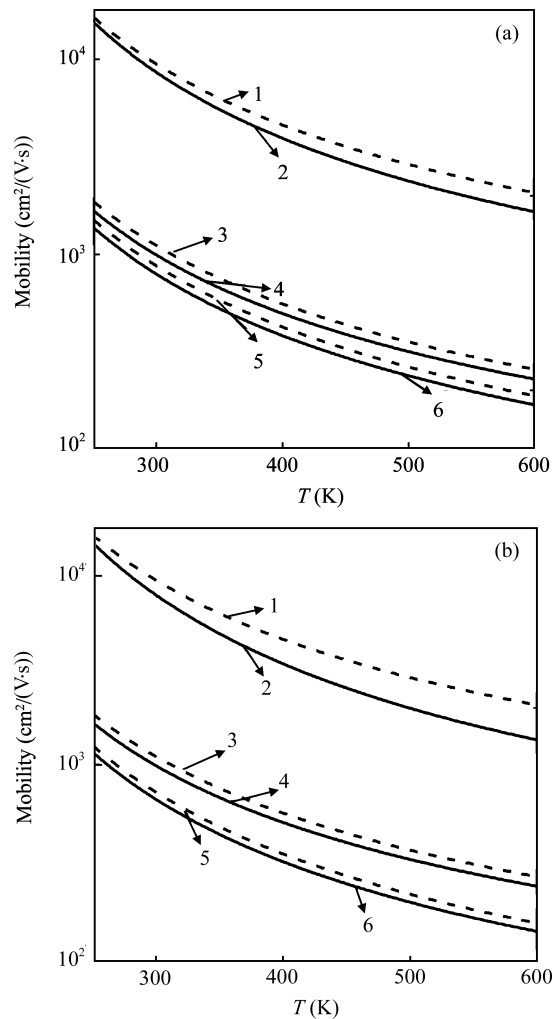| Material	a	$\varepsilon_{//}^{\infty} = \varepsilon_{z}^{\infty}$	f_{I}	m_z	$m_{//}$	C_{11}	C_{12}	C_{13}	C_{33}
GaN	3.189[a]	5.35[b]	0.5[c]	0.20[d]	0.20[d]	3900[a]	1450[a]	1060[a]	3980[a]
AlN	3.122[a]	4.84[b]	0.449[c]	0.32[d]	0.28[d]	3980[a]	1400[a]	1270[a]	3820[a]

[a]Ref. [16], [b]Ref. [17], [c]Ref. [18], [d]Ref. [19].

Table 2. Physical parameters of wurtzite GaN and AlN. The energy is in units of meV, the phonon frequencies in cm^{-1}, and the pressure coefficients in meV/kbar.

Material	E_{g}	$\omega_{//L}$	$\omega_{//T}$	ω_{zL}	ω_{zT}	$\gamma_{//L}$	$\gamma_{//T}$	γ_{zL}	γ_{zT}	α
GaN	3507[d]	757[e]	568[e]	748[e]	540[e]	0.99[e]	1.19[e]	0.98[e]	1.21[e]	3.6[f]
AlN	6230[d]	924[e]	677[e]	898[e]	618[e]	0.91[e]	1.18[e]	0.82[e]	1.02[e]	4.7[f]

[e]Ref. [1], [f]Ref. [20].

Fig. 1. Mobility versus temperature for given $n_s = 2 \times 10^{12}$ cm^{-2}. The curves for an unstrained (strained) heterojunction are 1(2): IF, 3(4): HS, 5(6): IF + HS, respectively. Experimental result (square point) is given from Ref. [21] for comparison.

channel is weakened and that from the IF ones is enhanced. However, the latter is not important compared with the former. Meanwhile, conduction band bending becomes unnoticeable, and the value of the electron–phonon matrix becomes bigger due to the modification of strain to the electronic effective masses and dielectric constants. As a result, both IF and HS phonon scattering are strengthened to decrease the total mobility significantly. The calculated result of electronic mobility is 810 cm^2/(V·s) for the strained case at 300 K; this is slightly lower than the value given by experiment (1015 cm^2/(V·s) when $n_s = 1.1 \times 10^{13}$ cm^{-2})$^{[21]}$ since variation in AlN thickness and electronic density can influence the electronic mobility. The calculation for a finite barrier or channel with higher electronic densities will be the subject of future work.

The electronic mobility in an unstrained heterojunction as a function of temperature T for a given electric density $n_s = 2 \times 10^{12}$ cm^{-2} is calculated by taking the scattering from the IF and HS phonon modes into account. As shown in Fig. 2(a) ($P = 200$ kbar) and Fig. 2(b) ($P = 400$ kbar), hydrostatic pressure also obviously reduces the electronic mobility, and the reduction increases continually as T increases.

Fig. 2. Mobility versus temperature at (a) 200 kbar and (b) 400 kbar for given $n_s = 2 \times 10^{12}$ cm^{-2} in an unstrained heterojunction. The curves without pressure (with pressure) are 1(2): IF, 3(4): HS, 5(6): IF+HS, respectively.

Comparing the numerical result without pressure to that with pressure $P = 200$ kbar and $P = 400$ kbar, it can be seen that the net decreases of the mobility are by 18.1% and 30% for $T = 300$ K, and by 26.2% and 42.5% for $T = 600$ K, respectively. The energy gaps in both materials increase with P, and the increase in the barrier is larger than that in the channel, so the potential height will gradually increase with P to repulse
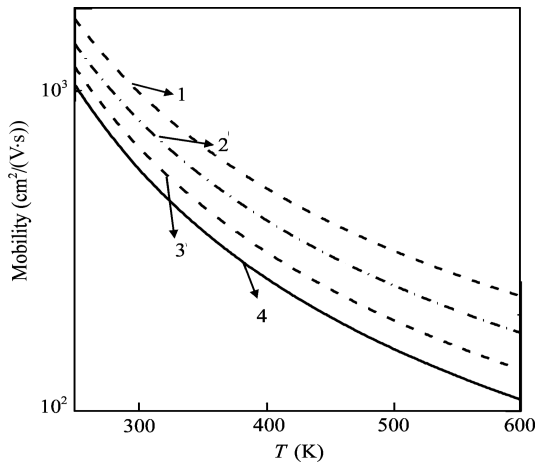
Fig. 3. Mobility versus temperature for given $n_s = 2 \times 10^{12}$ cm^{-2}. The curves are 1: without pressure and strain, 2: with strain and $P = 0$ kbar, 3: with strain and $P = 200$ kbar, 4: with strain and $P = 400$ kbar, respectively.
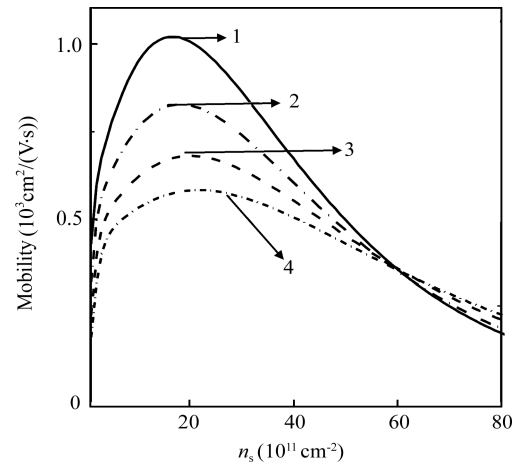

Fig. 4. Mobility versus electronic density for given $T = 300$ K. The curves are 1: without pressure and strain, 2: with strain and $P = 0$ kbar, 3: with strain and $P = 200$ kbar, 4: with strain and $P = 400$ kbar, respectively.

electrons moving. towards the channel. As a result, scattering from HS phonon modes in the channel becomes stronger. Meanwhile, the electronic effective masses increase, whereas the high frequencies and static dielectric constants decrease due to P. Conduction band bending becomes more noticeable and the value of the electron–phonon interaction matrix increases to strengthen the scattering from both the IF and HS phonon modes, and the influence from pressure on the HS phonon modes is more significant than that on the IF phonon modes. Consequently, electronic mobility obviously decreases.

The total electronic mobility as a function of temperature is shown by Fig. 3 for $n_s = 2 \times 10^{12}$ cm^{-2}. As mentioned above, both the pressure and strain decrease the electronic mobility, but the influence from pressure on the mobility with strain is smaller than that without strain since the compressive strain in the channel compensates the pressure effect. The net decrease of the mobility is by 38% at $T = 600$ K and $P = 400$ kbar, compared to that with strain and without pressure. It is also found that electronic mobility decreases obviously as the temperature increases, no matter whether strain and hydrostatic pressure exist, since the lattices oscillate strongly at high temperatures to increase the scattering from phonons.

Figure 4 presents the total mobility in strained and unstrained heterojunctions as a function of electronic density n_s at $T = 300$ K under different P, respectively. It can be seen that the total mobility first increases and then decreases significantly as n_s increases. The tendency of corresponding curves for a strained heterojunction under different P is the same as that for an unstrained one without pressure. This results from the fact that the confinement of the electrons in the channel and the correlation of the electrons are functions of n_s. At lower n_s, confinement and correlation are both weak. The mobility is determined mainly by strong scattering from the HS phonon modes. Increasing n_s induces band bending so that the average distance between an electron and the interface decreases. Scattering from the IF phonons becomes slightly stronger but

it cannot counteract the decrease of scattering from the HS phonons so the total mobility has a maximum value in Fig. 4. At this moment, scattering from the HS phonon modes has main responsibility for the total mobility. The strong correlation of the electrons obviously reduces the mobility as n_s increases from a larger value, and this phenomenon agrees qualitatively with what was found in experiment[23]. Scattering from the HS phonons is still dominant in deciding the mobility although the average distance of the 2DEG to the interface becomes smaller. It can be seen that both strain and hydrostatic pressure reduce the increase of the mobility at a smaller n_s, while they reduce its decrease when n_s is larger than 1.8×10^{12} cm^{-2}. The reason for this has been discussed above for a smaller n_s. For a larger n_s, the decrease of the correlation between electrons due to the modulation of strain and hydrostatic pressure plays a dominant role in raising mobility compared with that without modulation.

4. Conclusions

The effect of strain and hydrostatic pressure on electronic mobility influenced by optical-phonon modes in wurtzite AlN/GaN heterojunctions is discussed. It is shown that both strain and hydrostatic pressure will reduce the mobility when the electronic density varies within a certain range, but the influence of hydrostatic pressure on the mobility becomes weaker because of the modulation of strain. The effect of strain and pressure becomes more obvious as temperature increases. It is also shown that scattering from half space phonon modes in the channel side plays a dominant role in the mobility. The total mobility first increases and then decreases significantly, whereas the strain and hydrostatic pressure reduce this trend as the electronic density increases.

References

[1] Wagner J M, Bechstedt F. Pressure dependence of the dielectric and lattice-dynamical properties of GaN and AlN. Phys Rev B,

2000, 62(7): 4526

[2] Goñi A R, Siegle H, Syassen K, et al. Effect of pressure on optical phonon modes and transverse effective charges in GaN and AlN. Phys Rev B, 2001, 64(3): 035205

[3] Consejo C, Konczewicz L, Contreras S, et al. High pressure study of the electrical transport phenomena in AlGaN/GaN heterostructures. Phys Status Solidi B, 2003, 235(2): 232

[4] Łepkowski S P. Nonlinear elasticity effect in group III-nitride quantum heterostructures: *ab initio* calculations. Phys Rev B, 2007, 75(19): 195303

[5] Jia X M, Ban S L. Optical phonon influence on the mobility of electrons in wurtzite and zincblende AlN/GaN quantum wells. J Physics: Conference Series, 2007, 92: 012065

[6] Hasbun J E, Ban S L. Optical-phonon scattering in quasi-two-dimensional heterojunction systems. Phys Rev B, 1998, 58(4): 2102

[7] Nardelli M B, Rapcewicz K, Bernholc J. Strain effects on the interface properties of nitride semiconductors. Phys Rev B, 1997, 55(12): R7323

[8] Lee B C, Kim K W, Stroscio M A, et al. Optical-phonon confinement and scattering in wurtzite heterostructures. Phys Rev B, 1998, 58(8):4860

[9] Lei X L, Ting C S. Green's-function approach to nonlinear electronic transport for an electron-impurity-phonon system in a strong electric field. Phys Rev B, 1985, 32(2): 1112

[10] Shan W, Hauenstein R J, Fischer A J, et al. Strain effects on excitonic transitions in GaN: Deformation potentials. Phys Rev B, 1996, 54(19): 13460

[11] Ting D Z Y, Chang Y C. $\Gamma - X$ mixing in GaAs/Al$_x$Ga$_{1-x}$As and Al$_x$Ga$_{1-x}$As/AlAs superlattices. Phys Rev B, 1987, 36(8): 4359

[12] Piotr P, Laila M, Naud A, et al. Reduction of the energy gap pressure coefficient of GaN due to the constraining presence of the sapphire substrate. J Appl Phys, 1999, 85(4): 2385

[13] Wagner J M, Bechstedt F. Properties of strained wurtzite GaN and AlN: *ab initio* studies. Phys Rev B, 2002, 66(11): 115202

[14] Goñi A R, Syassen K, Cardona M. Effect of pressure on the refractive index of Ge and GaAs. Phys Rev B, 1990, 41(14): 10104

[15] Holtz M, Seon M. Pressure dependence of the optic phonon energies in Al$_x$Ga$_{1-x}$As. Phys Rev B, 1996, 54(12): 8714

[16] Park S H, Chuang S L. Comparison of zinc-blende and wurtzite GaN semiconductors with spontaneous polarization and piezoelectric field effects. J Appl Phys, 2000, 87(1): 353

[17] Bungaro C, Rapcewica K, Bernholc J. *Ab initio* phonon dispersions of wurtzite AlN, GaN and InN. Phys Rev B, 2000, 61(10): 6720

[18] Yarub A D. Electronic and positron properties of zinc-blende structure of GaN, AlN and their alloy Ga$_{1-x}$Al$_x$N. J Appl Phys, 2003, 93(12): 9730

[19] Vurgaftmana I, Meyer J R, Rarnmohan L R. Band parameters for III–V compound semiconductors and their alloys. J Appl Phys, 2001, 89(11): 5815

[20] Wei S H, Zunger A. Predicted band-gap pressure coefficients of all diamond and zinc-blende semiconductors: chemical trends. Phys Rev B, 1999, 60(8): 5404

[21] Hubbard S M, Pavlidis D, Valiaev V, et al. Metal-organic vapor phase epitaxy growth and characterization of AlN/GaN heterostructures. J Electron Mater, 2002, 31(5): 395

[22] Bai X P, Ban S L. Pressure effect on electronic mobility in quasi-two-dimensional AlGaAs/GaAs heterojunction systems. Chinese Journal of Semiconductors, 2005, 26(12): 2422

[23] Ambacher O, Smart J, Shealy J R, et al. Two dimensional electron gases induced by spontaneous and piezoelectronic polarization charge in N- and Ga-face AlGaN/GaN heterostructures. J Appl Phys, 1999, 85(6): 3222